SIMULACIÓN DE LA DISPERSIÓN DE SUSTANCIAS TÓXICAS MEDIANTE CFD

Simulation of toxic substance dispersion using CFD

Luis G. Zárate [*]
Mario E. Cordero [†]
Aleydis Ponce [‡]
Arturo E. Escartín [§]

Resumen

El estudio aborda la simulación de la dispersión atmosférica de sustancias tóxicas, específicamente amoníaco, utilizando la Dinámica de Fluidos Computacional (CFD). Se emplea el software COMSOL 6.2 para modelar la dispersión en dos y tres dimensiones, aplicando modelos de turbulencia k-ε y LES, junto con el modelo de Transporte de especies diluidas. La investigación se centra en la hidrodinámica de flujos turbulentos y la dispersión química, considerando las complejidades y no linealidades que estos fenómenos presentan. Los resultados muestran la evolución de una nube tóxica de amoníaco, destacando la importancia de la CFD para prever comportamientos y apoyar la toma de decisiones en situaciones de emergencia. Las simulaciones 3D resaltan los desafíos en la predicción precisa debido a las variaciones de velocidad y concentración en diferentes puntos del dominio. En conclusión, aunque la CFD es una herramienta poderosa, existen limitaciones significativas que aún requieren investigación para mejorar la precisión y eficacia en la gestión de emergencias químicas.

Palabras Clave: *Dispersión atmosférica, amoníaco, CFD, simulación, modelado numérico, emergencia química.*

Abstract

The study addresses the simulation of atmospheric dispersion of toxic substances, specifically ammonia, using Computational Fluid Dynamics (CFD). COMSOL 6.2 software is employed to model the dispersion in two and three dimensions, applying k-ε turbulence models and Large Eddy Simulation (LES), along with the Transport of Diluted Species model. The research focuses on the hydrodynamics of turbulent flows and chemical dispersion, considering the complexities and nonlinearities of these phenomena. The results show the evolution of a toxic ammonia cloud, highlighting the importance of CFD in predicting behaviors and supporting decision-making in emergency situations. The 3D simulations emphasize the challenges in accurate prediction due to variations in velocity and concentration at different points within the domain. To summarize, although CFD is a powerful tool, significant limitations remain that require further research to improve accuracy and effectiveness in managing chemical emergencies.

Keywords: *Atmospheric dispersion, ammonia, CFD, simulation, numerical modeling, chemical emergency.*

[*] Luis G. Zárate luis.zarate@upaep.mx
[†] Mario E. Cordero marioedgar.cordero@upaep.mx
[‡] Aleydis Ponce aleydis.ponce@upaep.edu.mx
[§] Arturo E. Escartín arturoeduardo.escartin@upaep.edu.mx

1 Introduction

In historical analyses of major accidents (toxic leaks, atmospheric dispersals, fires, explosions), it can be observed that most containment losses occur due to spills and leaks (81%), followed by fires (9.7%) and explosions (8.8%); this information is depicted in Fig. 1 [5]. These observations are based on 15,841 records compiled by the Federal Attorney for Environmental Protection (PROFEPA) between 2000 and 2014 across Mexico's 32 federal entities. It is also noted that the majority of accidents occur during the transportation of chemical substances through pipelines and roads (together accounting for 97.8%

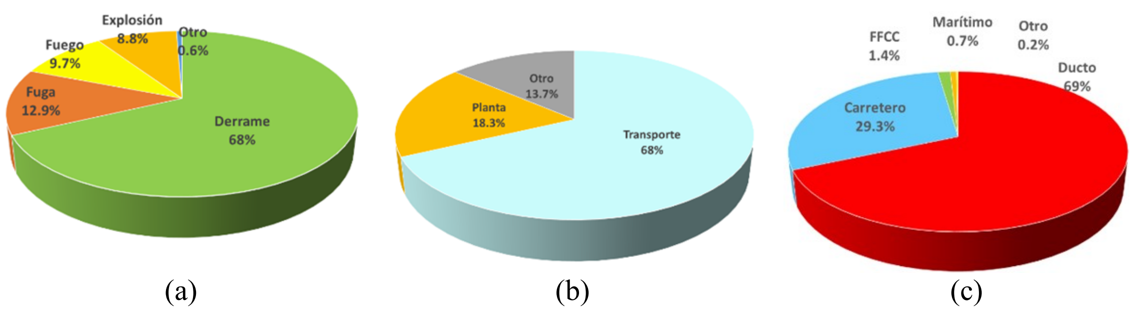

Fig. 1 Chemical Emergencies recorded by PROFEPA from 2000 to 2021. a) Distribution of emergencies considered as major accidents. b) Location of the accident. c) Environment where they occur.

In other publications of environmental emergency statistics [1], the record compiled by PROFEPA (CENAPRED 2014) for the period from 2010 to 2014 is reported, during which a total of 2835 chemical emergencies occurred. Table 1 shows the top ten substances among over 440 substances involved in these chemical emergencies. Based on this information, it can be stated that the potential scenarios for various cases are countless, translating into an impressive number of variables, highlighting the significant difficulty in studying and replicating accident conditions and variations—virtually impossible to reproduce experimentally. Within this framework, mathematical modeling and simulation become crucial, with this discipline abstracting a phenomenon through one or multiple mathematical equations to predict the behavior of the modeled system. These techniques allow the study of multiple and varied conditions, different geometries, and variations in significant variables without accident risks and in an economical manner [6]. It is also necessary to note that while such studies are feasible through numerical approximation techniques, the complexity of the phenomena leads to nonlinear behaviors, requiring substantial computational resources, which pose limitations. This work, due to its scientific robustness, focuses on studying chemical dispersion using CFD modeling and simulation to analyze the behavior of an ammonia toxic cloud.

Table 1. Substances involved in chemical emergencies from 2010 to 2014

Substance	Percentage %	Cumulative %
Crude oil	24.42	24.42
Gasoline	11.71	36.13
Diesel	10.21	46.34
Fuel oil	5.91	52.25
Liquefied petroleum gas	4.11	56.36
Natural gas	3.57	59.93
Ammonia	3.42	63.35
Gunpowder	1.92	65.27
Sulfuric acid	1.66	66.93
Jet fuel (Turbosina)	1.36	68.29
Other substances (446)	31.71	100
Source: CENAPRED (2014)		

CFD

Computational Fluid Dynamics (CFD) is a methodology that utilizes computational tools to solve mathematical models of mass, momentum, and energy conservation in their differential forms to understand fluid behavior considering possible changes in time and space (see Table 2). This finds wide application across various disciplines such as Engineering, Energy, Mathematics, Materials Science, Computer Science, Environmental Science, etc. Fatnassi searched for the term

Table 2. Mathematical models of mass, momentum, and heat transport used in Computational Fluid Dynamics (CFD)	
Moment $\rho\frac{\partial \mathbf{u}}{\partial t}+\rho(\mathbf{u}\cdot\nabla)\mathbf{u}=\nabla\cdot\left[-p\mathbf{I}+(\mu+\mu_T)\left(\nabla\mathbf{u}+(\nabla\mathbf{u})^T-\frac{2}{3}(\mu+\mu_T)(\nabla\mathbf{u})\mathbf{I}\right)\right]+\mathbf{F}$ $\rho\frac{\partial \mathbf{u}}{\partial t}+\nabla\cdot(\rho\mathbf{u})=0$	**Energy** $\rho C_P\frac{\partial T}{\partial t}+\rho C_P\mathbf{u}\cdot\nabla T+\nabla\mathbf{q}=Q_{gen}$ $\mathbf{q}=-k\nabla T;\quad Q_{gen}=-\Delta H_{rxn}R_i$
Turbulence Model $\kappa-\varepsilon$ $\rho\frac{\partial \kappa}{\partial t}+\rho(\mathbf{u}\cdot\nabla)\kappa=\nabla\cdot\left[\left(\mu+\frac{\mu_T}{\sigma_\kappa}\right)\nabla\kappa\right]+P_\kappa-\rho\varepsilon$ $\rho\frac{\partial \varepsilon}{\partial t}+\rho(u\cdot\nabla)\varepsilon=\nabla\cdot\left[\left(\mu+\frac{\mu_T}{\sigma_\varepsilon}\right)\nabla\varepsilon\right]+C_{\varepsilon1}\frac{\varepsilon}{\kappa}P_\kappa-C_{\varepsilon2}\rho\frac{\varepsilon^2}{\kappa};\quad \varepsilon=ep$ $\mu_T=\rho C_\mu\frac{\kappa^2}{\varepsilon};\quad P_\kappa=\mu_T\left[\nabla\mathbf{u}:\left(\nabla\mathbf{u}+(\nabla\mathbf{u})^T\right)-\frac{2}{3}(\nabla\cdot\mathbf{u})^2\right]-\frac{2}{3}\rho\kappa\nabla\cdot\mathbf{u}$ LES model $\rho\frac{\partial(u+u')}{\partial t}+\nabla\cdot(\rho uu^T+\rho uu'^T+\rho u'u^T+\rho u'u'^T+p'I)=\nabla\cdot[-pI+K]+F+\rho g$ $\rho\nabla\cdot(u+u')=0$ $K=\mu(\nabla(u+u')+(\nabla(u+u'))^T)-\frac{2}{3}\mu(\nabla\cdot(u+u'))I$	**Mass** $\frac{\partial c_i}{\partial t}+\nabla\cdot(-D_i\nabla c_i)+\mathbf{u}\cdot\nabla c_i=R_i$ $\mathbf{N}_i=-D_i\nabla c_i+\mathbf{u}c_i$
Selection of some of the variables and parameters used in the models	
•Velocity, u •Time, t •Pressure, p •Dynamic viscosity, μ •Kinetic energy, k (turbulence model) •Thermal conductivity, k (energy model) •Turbulent dissipation rate, ε •Volume force, F •Gravity, g	•Energy generation, Q_{gen} •Specific heat capacity, Cp •Heat reaction, H •Temperature, T •Reaction rate for the species i, R_i •Diffusion coefficient, D_i •Species concentration i, c_i

"Computational Fluid Dynamics" in the Scopus database, yielding over 90,000 articles [2]. This highlights the significance and extensive use of CFD even today. Moreover, it continues to evolve and integrate advances in the foundational sciences.

Regarding Risk Analysis, publications are found on the study of atmospheric dispersion, different types of fires, explosions, and problem resolution related to fluid hydrodynamics and mass transport, solving various models as shown in Table 2. Through numerical methods techniques, which couple and solve simultaneously, in steady-state or time-dependent conditions, with possible chemical reactions and energy release. As mentioned earlier, Computational Fluid Dynamics (CFD) is widely used in simulating the dispersion of toxic substances in the environment, primarily in applications such as emergency responses and chemical, bioaerosol, and radionuclide modeling; playing an increasingly important role in emergency planning and response, though significant uncertainties remain to be addressed, there is consensus that it is a critically important tool that can effectively contribute to understanding real or hypothetical situations, supporting decision-making [7]. This study employs this tool to investigate an ammonia dispersion. It focuses on this compound because its production and use are continuously growing, and it can be found in any country worldwide, being essential in various every day and industrial applications, such as fertilizer industry, nitric acid production, subsequently processed for explosives, fibers, plastics, dyes, pharmaceuticals, and ammonium nitrate; other uses include chemical compound production for selective catalytic reduction (SCR) systems, refrigeration units, wastewater treatment, metal treatment, leather, rubber, paper, household cleaning, food, and beverage industries [4]. While the above is true, and ammonia is a highly useful chemical compound, it should also be noted that it poses significant risks, such as respiratory toxicity, ocular and dermal irritation, and hazards related to hydrogen gas release, emphasizing the need for careful handling.

Table 3. Summary of the threshold values that serve as guidance for exposure (AEGL) to ammonia over various time periods and their health effects [3].

Classification	**Exposure Time and Concentrations (in ppm and mg*m^-3)**				
	10 min	**30 min**	**1 h**	**4 h**	**8 h**
AEGL-1 No incapacitates	30 ppm 21 mg/m3	30 ppm 21 mg/m3	30 ppm 21 mg/m3	30 ppm 21 mg/m3	30 ppm 21 mg/m3
AEGL-2 Incapacitates	220 ppm 154 mg/m3	220 ppm 154 mg/m3	160 ppm 112 mg/m3	110 ppm 77 mg/m3	110 ppm 77 mg/m3
AEGL-3 Lethal	2700 ppm 1888 mg/m3	1600 ppm 1119 mg/m3	1100 ppm 769 mg/m3	550 ppm 385 mg/m3	390 ppm 273 mg/m3

Source: National Research Council (2008).

In Table 3, a classification of effects on individuals is presented, ranging from mild irritation for AEGL-1, considered disabling for AEGL-2 due to causing irritation of eyes, throat, and inducing coughing. Meanwhile, AEGL-3 category represents a lethal exposure [3].

2 Methodology

COMSOL 6.2 software is utilized for simulating the atmospheric dispersion of ammonia in both 2D and 3D. To address hydrodynamics, the k-ε turbulence models and Large Eddy Simulation (LES) are employed. For mass transport, the Transport of Diluted Species model is used, as detailed in Table 2. Fig. 2 presents some of the geometries examined. For the 2D domain, a height of 12 meters and a length of 1000 meters were assigned, with amplification of the region where the toxic substance is released, as the 2-inch diameter of the leaking ammonia tube is not discernible against the 1000-meter length. For the 3D simulations, as depicted in Fig. 3, the domain was reduced due to the significant computational requirements.

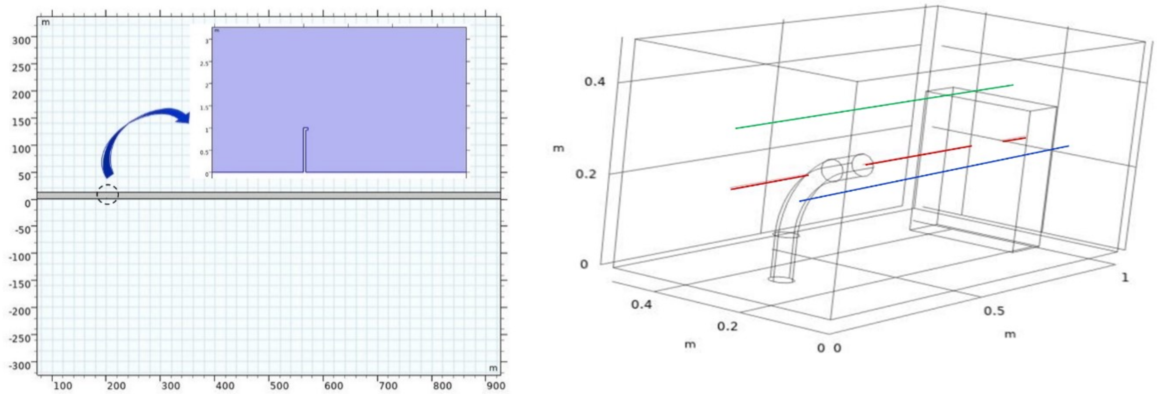

(a) (b)

Fig. 2 Selected geometries for simulating ammonia dispersion. (a) 2-dimensional geometry, with an enlargement of the point where the leak occurs. (b) 3-dimensional geometry, with cutting planes at different positions.

In Fig. 2b, three lines of different colors are placed. One red line coincides with the center of the tube where the ammonia exits and extends until it encounters the wall placed in front, continuing beyond the obstacle to the end of the considered domain. Another green line is positioned above the wall, very close but without touching it, allowing it to start and finish traversing the entire simulated domain. The blue line also spans the entire domain but is offset from the center, running parallel to the red line. These lines are used to evaluate the variables that may result from the simulation across these lengths.

3 Results

Figure 3 depicts the dispersion over time, clearly showing the evolution of the toxic plume moving in the direction of the wind, with noticeable swirls near the origin point of the leak. This phenomenon is more evident in Fig. 4, illustrating the distribution of concentration values in mol/m3. It is also notable that the highest concentration is observed at the leak outlet.

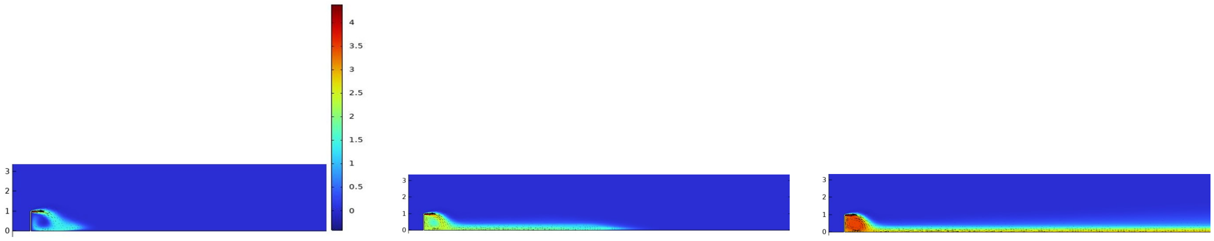

Fig. 3 Dispersion evolution with a concentration of 4.3 mol/m³ at the leak outlet

In Fig. 4, vectors are included to illustrate the flow direction of the chemical substance, along with the magnitude of variables such as velocity and concentration throughout the simulated domain. It should be noted that, despite the above, the behavior in depth or in the z-coordinate is unknown, which becomes significant when turbulence or obstacles are encountered in front of the dispersion; both cases are possible in major accidents. Therefore, simulations are conducted considering a scenario in 3 dimensions.

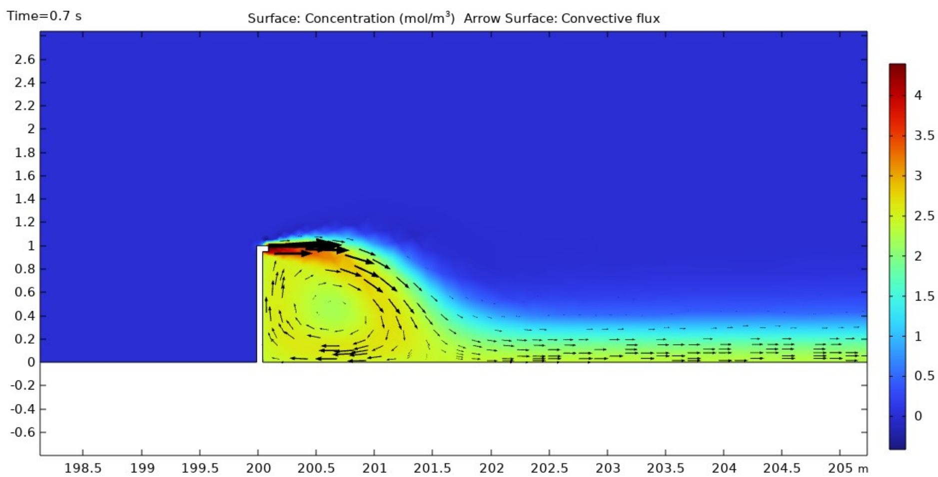

Fig. 4 Concentration and behavior of the released substance over time at 0.7 seconds.

3.1 Results for the 3D domain

Figure 5 presents the findings from the 3D simulation, where cutting planes are placed at coordinates yz, yx, and zx. Streamlines are also observed, and a color palette shows velocity values ranging from 0 m/s up to a maximum of 60 m/s, which are input conditions known to the simulator. Fig. 5(a) shows results at the simulation start (t=0s). Fig. 5(b) depicts results after 0.04s, and Fig. 5(c) after 2.9s.

In (a), initial conditions are observed with a velocity of 9 m/s. Streamlines only deviate from a linear behavior upon encountering the wall, deflecting upwards and sideways. Even in the central zone, there is movement opposite to the x-direction. In Fig. 5(b), a dart-like behavior is observed with maximum velocity values at the center of the exhaust pipe, decreasing as it moves away from the exit point. Upon reaching the wall, fluid passes around it, and in yx cuts, it can be seen that velocity is minimal at ground level but increases at higher levels, with fluid returning upon hitting the wall, resulting in a velocity magnitude in the x-direction opposite to that observed near the domain start or past the wall. Fig. 5(c) shows a similar pattern but with higher velocity magnitudes.

These findings present significant challenges in model resolution due to high values at the pipe exit, boundary layer observed on obstacle walls, various transition zones, laminar zone, and directional inversion in fluid impacting the obstacle. These variations and fluctuations introduce serious nonlinearity and convergence difficulties in numerical methods.

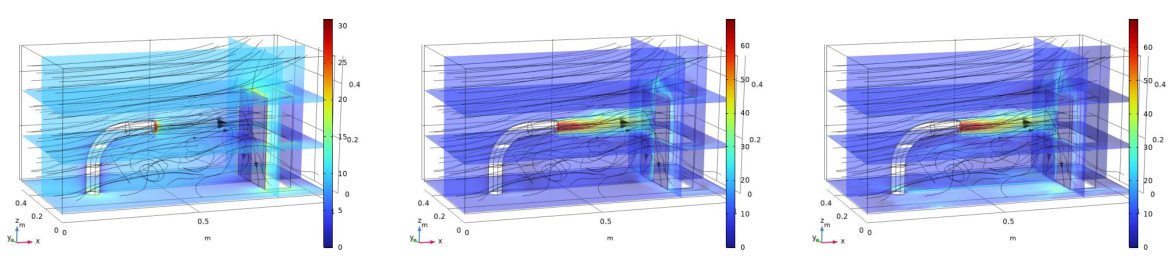

(a) t=0 s (b) t=0.04 s (c) t=2.9 s

Fig. 5 Hydrodynamic behavior of the 3D domain in a non-steady state.

In Figure 6, a graph is provided showing the velocity results along the lines mentioned in Fig. 2(b). Specifically, the solid lines represent velocity in the x-direction along the red line shown in Fig. 2(b). The asterisk-marked plots correspond to velocity values along the blue line, while the dashed lines with a small circle represent velocity results along the green line. Overall, the results exhibit expected behavior observed in reality, with maximum velocity occurring at the tube outlet, and entrance values along all three lines being 9 m/s, which were assigned at the inlet boundary. In areas where there is no domain due to the tube or wall, the result line is not observable. Near the wall, a boundary layer is observed with decreasing velocity values, occasionally reaching zero velocity, followed by an increase in velocity due to the influence of the leak jet, which adds to the velocity expected solely at the domain inlet.

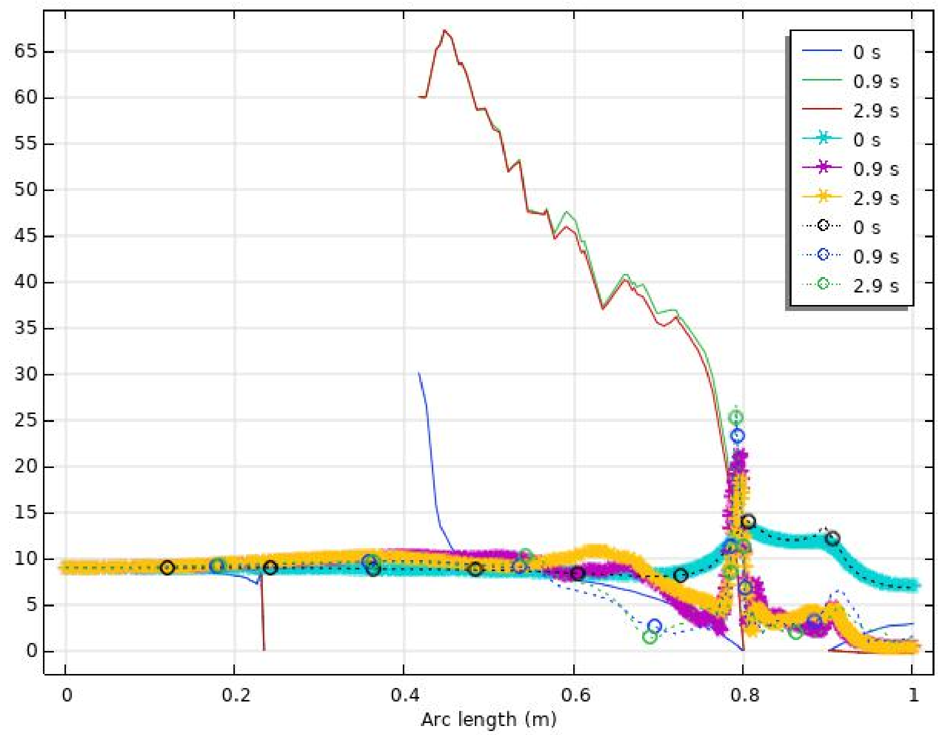

Fig. 6 Graph at different time instants of the velocity variable in the x-direction.

Past the wall, the trend is to recover the initial velocity value as it moves away from the point where an additional force is applied. It is evident that such movements contribute to convective mass transport, and with the presence of ammonia, this component will disperse in the direction of the flow (advective transport).

4 Conclusion

Despite significant advancements in safety within processes, storage, and transportation of chemicals, statistical analyses yield results that must be considered due to the high costs incurred when consequences occur. Moreover, these incidents can happen in uncertain conditions and locations, potentially affecting densely populated areas or facing entirely adverse conditions. Therefore, studying these accidents across various scenarios is crucial for prediction and, if possible, prevention. Computational Fluid Dynamics (CFD) proves to be a powerful tool in depicting accident behaviors, particularly in assessing the atmospheric dispersion of toxic and potentially lethal substances upon release.

The accuracy of these results is paramount in decision-making, as inaccuracies could lead to fatal outcomes. The hydrodynamics of turbulent flows and chemical dispersion involving possible chemical reactions are phenomena observed in major accidents. These phenomena pose a significant challenge to science due to their unstable, nonlinear behaviors and the multitude of variables beyond human control. Ongoing research in various fields holds promise, yet also underscores that uncertainties persist, influencing decisions and highlighting substantial limitations in predicting behaviors and consequently mitigating accidents.

References

1. Ania Mendoza Cantú A. e IZE LEMA I. A. R. (2017). Las sustancias químicas en México. Perspectivas para un manejo adecuado. Rev. Int. Contam. Ambie. (https://doi.org/10.20937/rica.2017.33.04.15)
2. Fatnassi Hicham, Bournet Pierre Emmanuel, Boulard Thierry, Roy Jean Claude, Molina-Aiz Francisco D., Zaaboul Rashyd (2023). Use of computational fluid dynamic tools to model the coupling of plant canopy activity and climate in greenhouses and closed plant growth systems: A review. Biosystems Engineering. (https://doi.org/10.1016/j.biosystemseng.2023.04.016)
3. National Research Council (2008). Acute Exposure Guideline Levels for Selected Airborne Chemicals: Volume 6. Washington, DC: The National Academies Press. (https://doi.org/10.17226/12018)
4. Nosherwani S. A., Costa Neto R. (2021) Techno-economic assessment of commercial ammonia synthesis methods in coastal areas of Germany. Journal of Energy Storage. (https://doi.org/10.1016/j.est.2020.102201)
5. PROFEPA (2022). Emergencias químicas en México. Procuraduría Federal de Protección al Ambiente [en línea] https://www.gob.mx/profepa/articulos/emergencias-quimicas-en-mexico
6. Ruiqing Shen, Zeren Jiao, Trent Parker, Yue Sun, Qingsheng Wang (2020). Recent application of Computational Fluid Dynamics (CFD) in process safety and loss prevention: A review. Journal of Loss Prevention in the Process Industries. (https://doi.org/10.1016/j.jlp.2020.104252)
7. Zhang X., Wang J. (2022). Atmospheric dispersion of chemical, biological, and radiological hazardous pollutants: Informing risk assessment for public safety. Journal of Safety Science and Resilience. (https://doi.org/10.1016/j.jnlssr.2022.09.001)

Caption List

Fig.1 Chemical Emergencies recorded by PROFEPA from 2000 to 2021. a) Distribution of emergencies considered as major accidents. b) Location of the accident. c) Environment where they occur.

Fig. 2 Selected geometries for simulating ammonia dispersion. (a) 2-dimensional geometry, with an enlargement of the point where the leak occurs. (b) 3-dimensional geometry, with cutting planes at different positions.

Fig. 3 Dispersion evolution with a concentration of 4.3 mol/m^3 at the leak outlet.

Fig. 4 Concentration and behavior of the released substance over time at 0.7 seconds

Fig. 5 Hydrodynamic behavior of the 3D domain in a non-steady state.

Fig. 6 Graph at different time instants of the velocity variable in the x-direction.